Supporting Information

Bimetallic-atoms improve Ni_3S_2 bifunctional electrocatalysts for efficient hydrogen evolution reaction and overall water splitting performance

Junjie Huang†, Lan Mu†, Yangyang Ou, Gang Zhao*, Jinzhao Huang, Xiao Wang, Baojie Zhang*

School of Physics and Technology, University of Jinan, Jinan 250022, China

* Corresponding address: sps_zhaog@ujn.edu.cn; zhangbaojie_ujn@163.com

†These authors contributed equally to this work.

Number of pages: 15

Number of figures: 11

Number of tables: 3

Table of contents

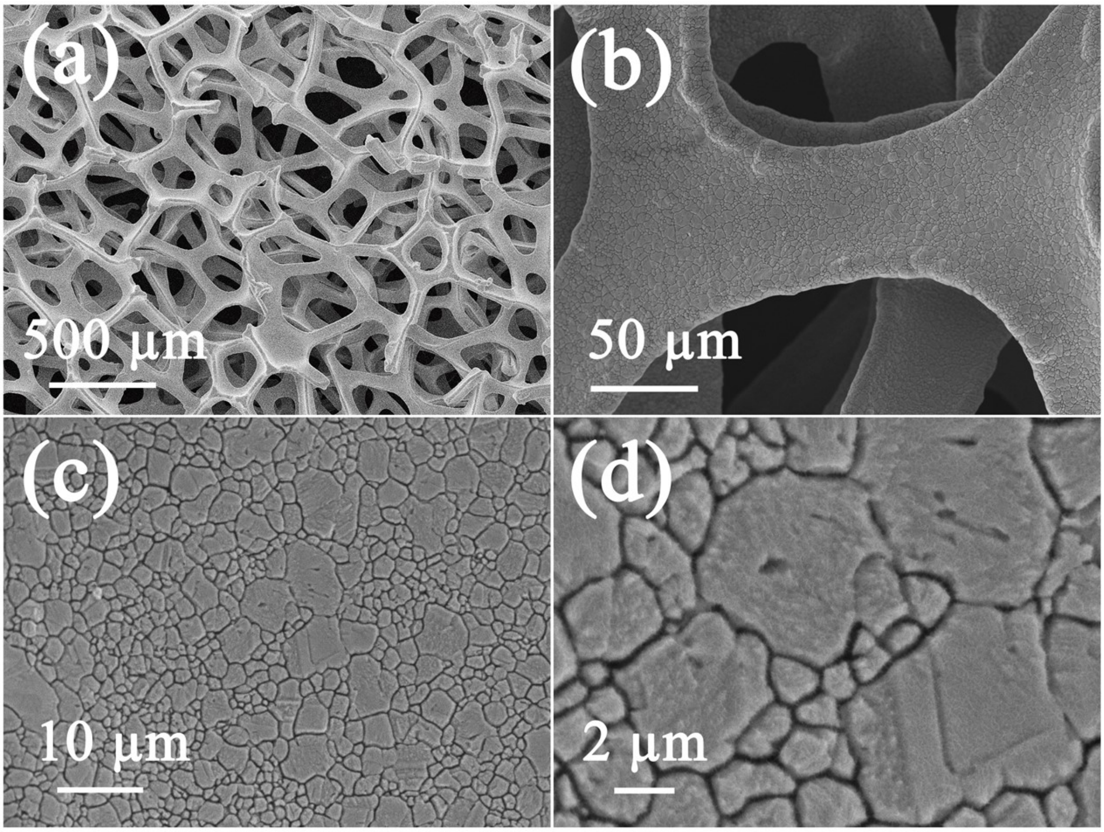

Fig. S1. (a-d) SEM images of bare nickel foam.

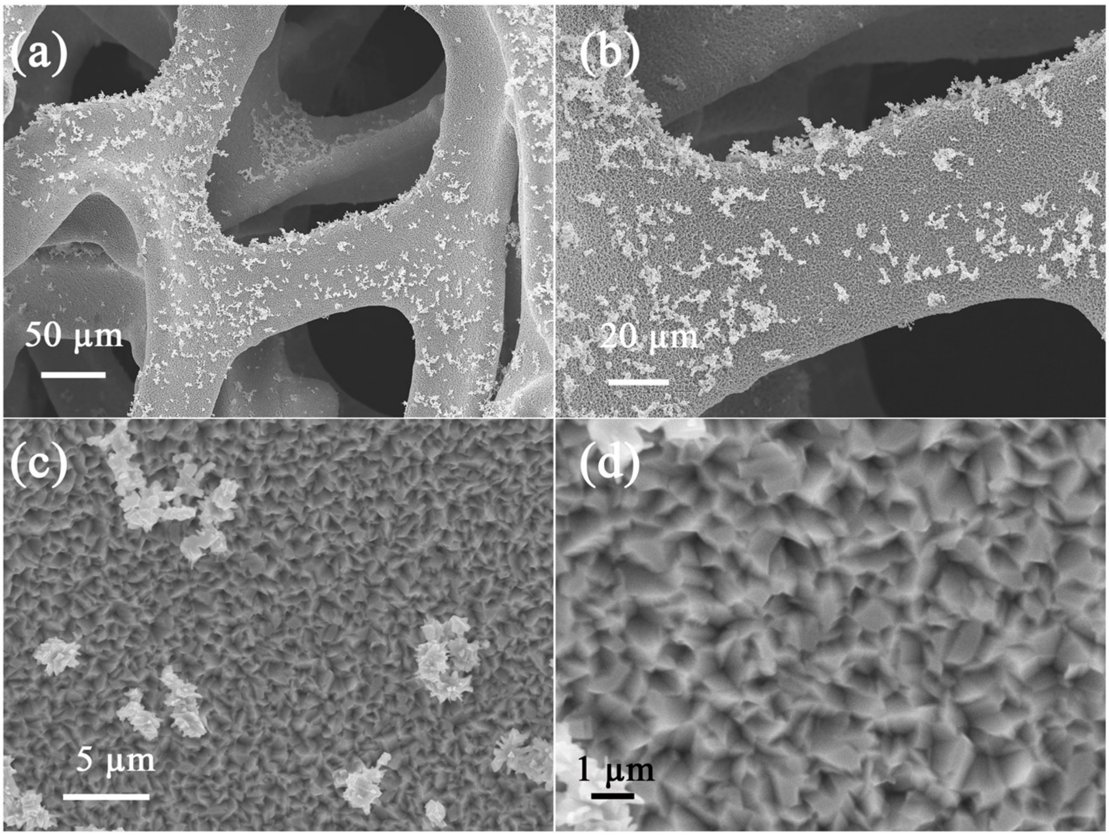

Fig. S2. (a,b,c,d)SEM images of Ni_3S_2.

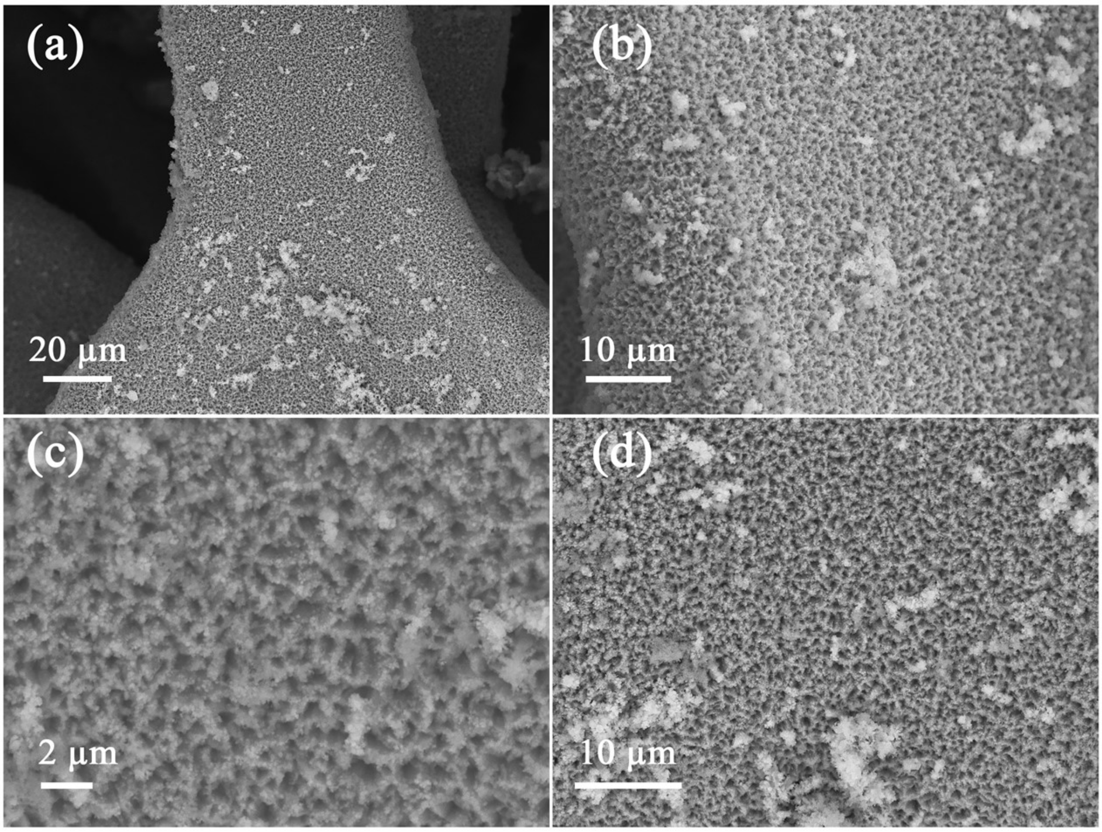

Fig S3. (a,b,c,d)SEM images of Ni_3S_2-Fe.

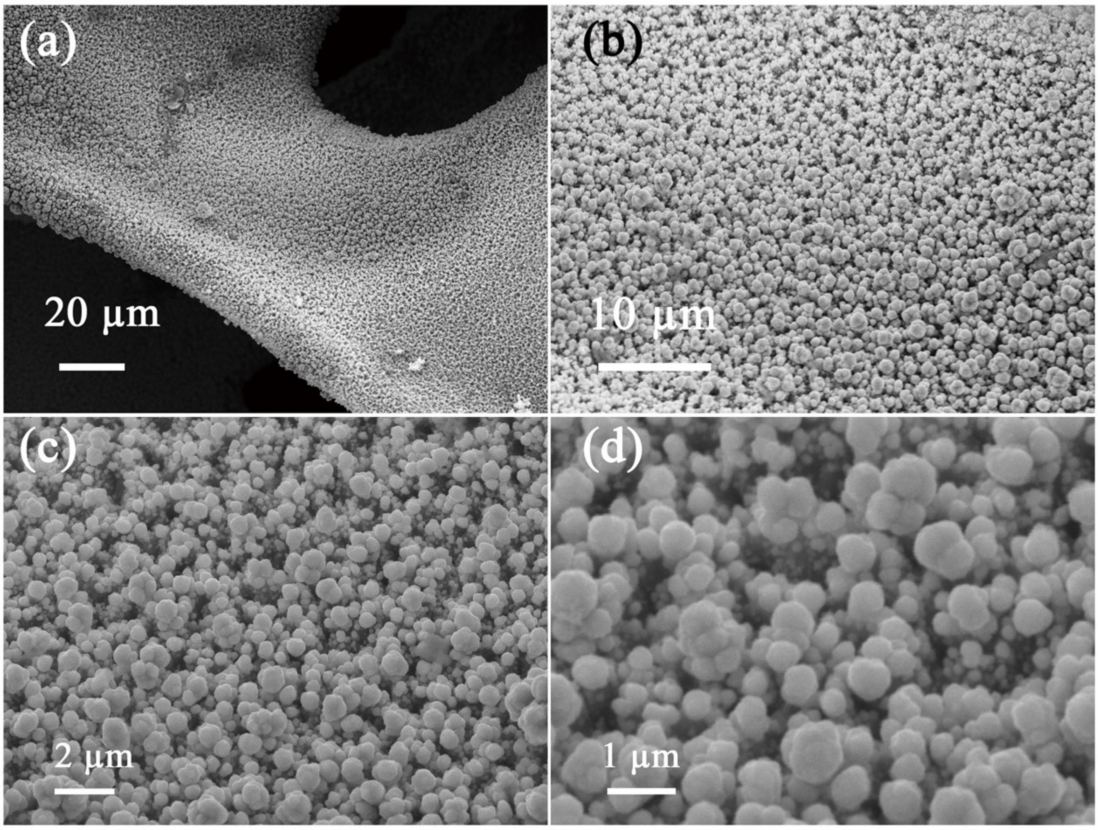

Fig. S4. (a,b,c,d)SEM images of Ni_3S_2-Fe-Ni.

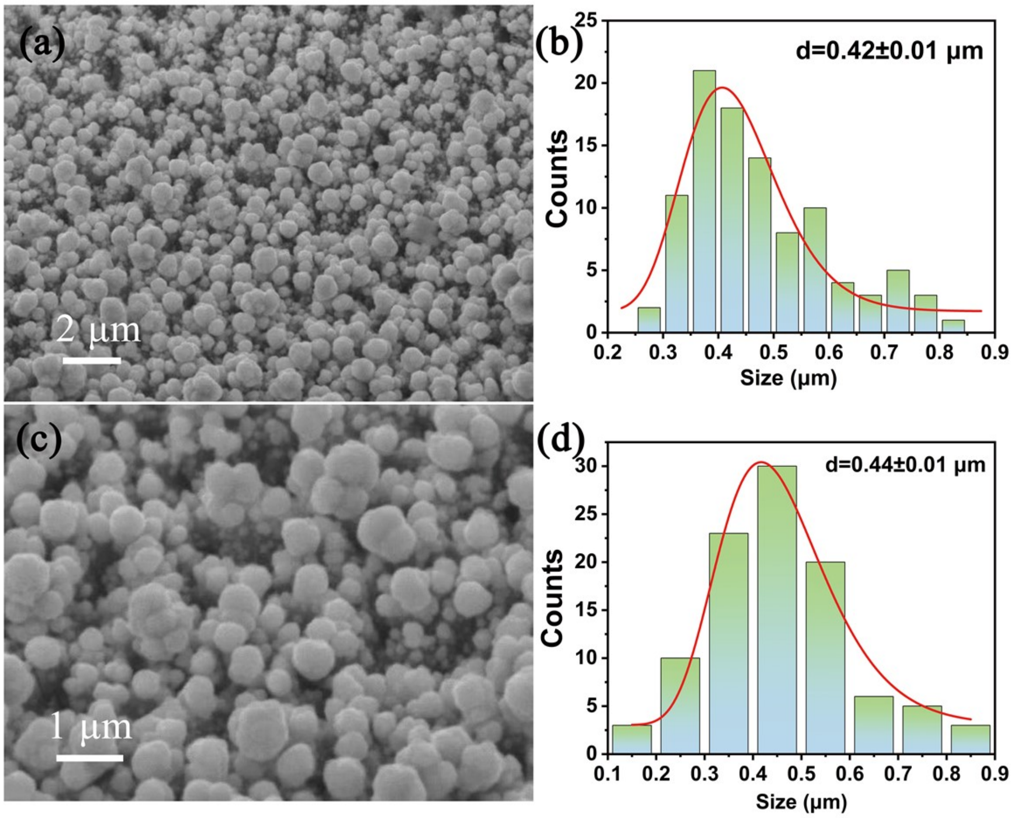

Fig. S5. (a,c) SEM images of Ni_3S_2-Fe-Ni_2. (b) Particle size analysis of (a). (d) Particle size analysis of (c).

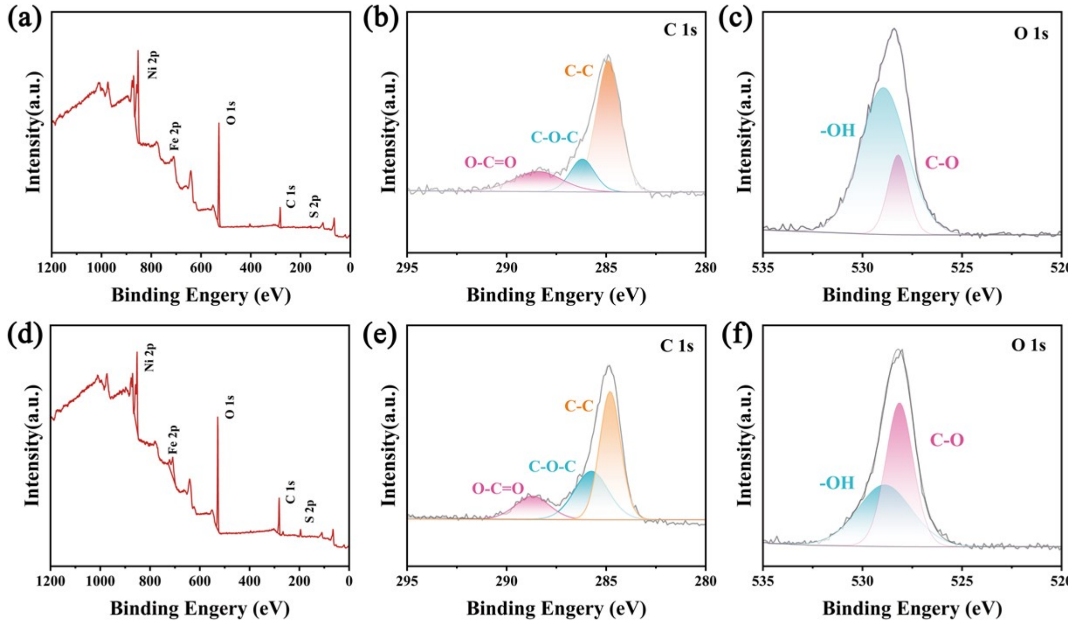

Fig. S6. XPS spectra of (a) survey. (b) C 1s. (c) O 1s for the Ni_3S_2-Fe. (d) survey. (e) C 1s. (f) O 1s for the Ni_3S_2-Fe-Ni.

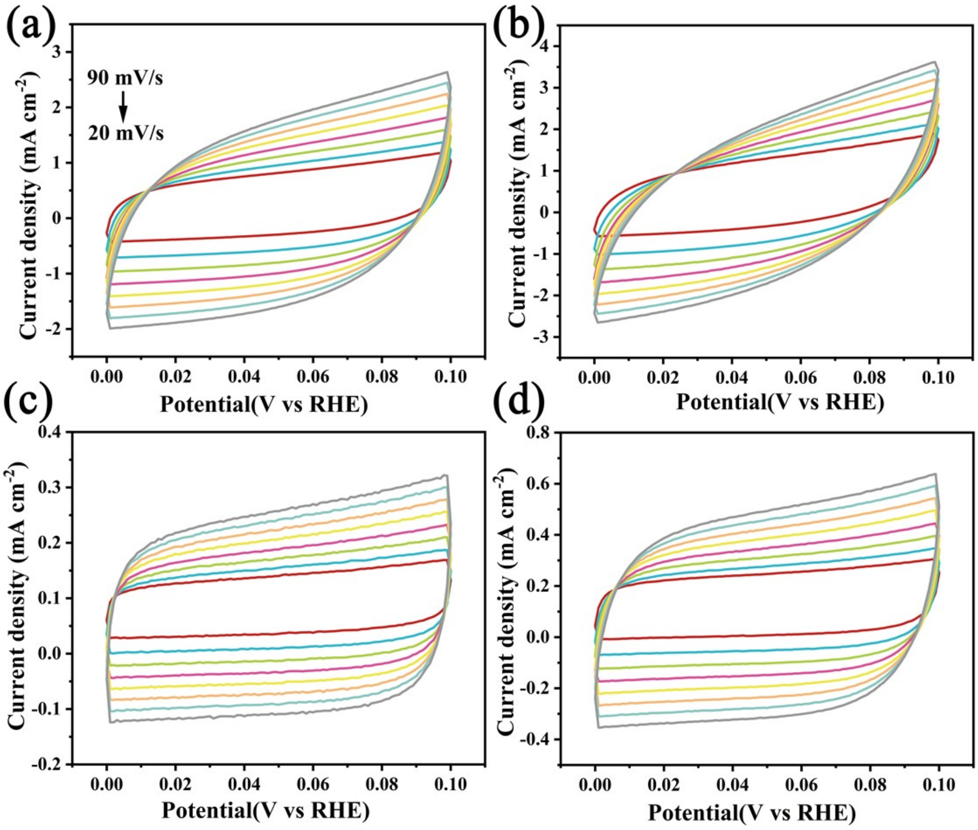

Fig. S7. (a) the double-layer capacitances of various catalysts CV curves at various scan rates of Ni_3S_2-Fe-Ni. (b) Ni_3S_2-Fe. (c) Ni_3S_2. (d) Ni.

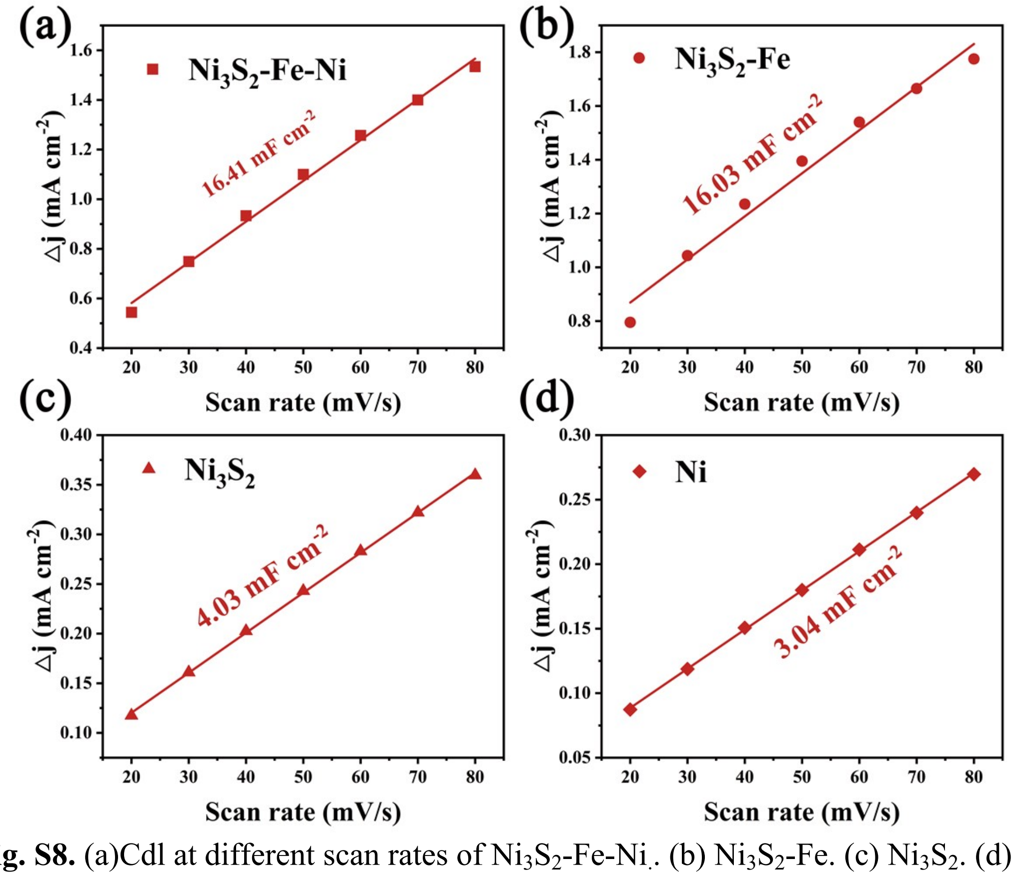

Fig. S8. (a)Cdl at different scan rates of Ni_3S_2-Fe-Ni. (b) Ni_3S_2-Fe. (c) Ni_3S_2. (d) Ni.

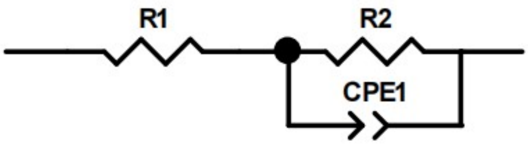

Element	Freedom	Value	Error	Error %
R1	Free(?	1.639	N/A	N/A
R2	Free(?	0.42283	N/A	N/A
CPE1-T	Free(?	0.15293	N/A	N/A
CPE1-P	Free(?	0.69853	N/A	N/A

Data File:	d:\desktop\OEREIS.txt
Circuit Model File:	
Mode:	Run Simulation / Freq. Range (0.001 - 1000000)
Maximum Iterations:	100
Optimization Iterations:	0
Type of Fitting:	Complex
Type of Weighting:	Calc-Modulus

Fig. S9. OER-EIS fitting data for Ni_3S_2-Fe-Ni

Element	Freedom	Value	Error	Error %
R1	Free(?	1.689	N/A	N/A
CPE1-T	Free(?	0.0054214	N/A	N/A
CPE1-P	Free(?	0.76774	N/A	N/A
R2	Free(?	2.203	N/A	N/A

Data File:	d:\desktop\HEREIS.txt
Circuit Model File:	
Mode:	Run Simulation / Freq. Range (0.001 - 1000000)
Maximum Iterations:	100
Optimization Iterations:	0
Type of Fitting:	Complex
Type of Weighting:	Calc-Modulus

Fig.S10. HER-EIS fitting data for Ni_3S_2-Fe-Ni

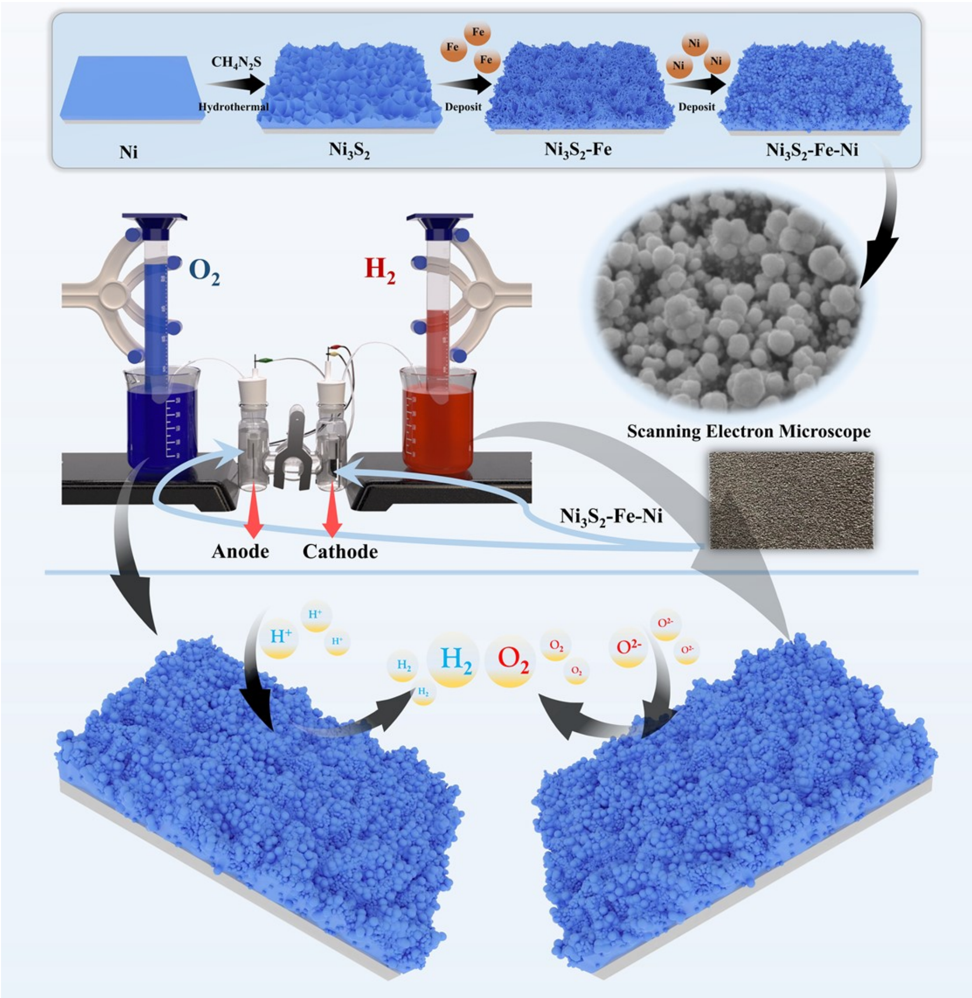

Fig. S11. Synthesis of overall-water-splitting materials and mechanism diagram

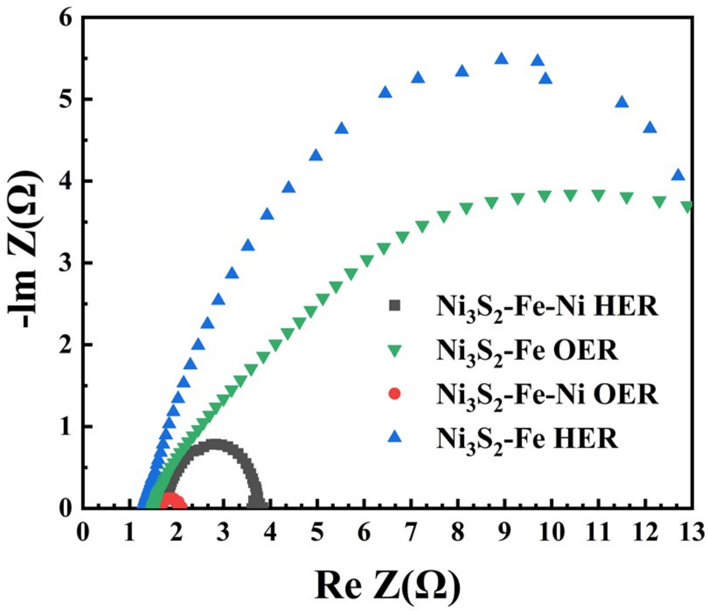

Fig. S12. original impedance diagram

Electrocatalysts	Electrolytes	Overpotential at 10 $mA \cdot cm^{-2}$ (mV)	
NiFe-LDHs/MXene/NF	1 M KOH	229	Nano Energy 63 (2019) 103880[1]
NiFe-LDHs/NF	1 M KOH	224	Chem. Sci. 6 (2015) 6624[2]
v-NiFe-LDHs	1 M KOH	210	Nano Energy 81 (2021) 105606[3]
NiFe-LDHs-V_{Ni}	1 M KOH	229	Small 14 (2018) 1800136[4]
NiFe-LDHs-NS@DG10	1 M KOH	210	Adv. Mater. 29 (2017) 1700017[5]
NiCoFe-LDHs	1 M KOH	288	ACS Catal. 10 (2020) 5179-5189[6]
NiFe-LDHs@NiCoP/NF	1 M KOH	220	Adv. Funct. Mater. 28 (2018) 1706847[7]
Ni_3S_2	**1 M KOH**	**363**	**This work**
Ni_3S_2-Fe	**1 M KOH**	**313**	**This work**
Ni_3S_2-Fe-Ni	**1 M KOH**	**190**	**This work**

Table S1. A comparison of the OER performances of recently reported electrocatalysts in alkaline electrolytes.

Electrocatalysts	Electrolytes	Overpotential at 10 $mA\cdot cm^{-2}$ (mV)	
Co@BNCNs	1M KOH	187	New Journal of Chemistry, 45 (2021) 6308-6314[8]
NC@Mo_2C@MoS_2-Ni	1M KOH	216	International Journal of Hydrogen Energy, 46 (2021) 5250-5258[9]
Ni_3S_2/NiS/NOSCs	1M KOH	180	ACS Sustainable Chemistry & Engineering, 6 (2018) 15582-15590[10]
rGO@Fe_3O_4	1M KOH	300	Journal of the Indian Chemical Society, 99 (2022) 100442[11]
CoP(MoP)-$CoMoO_3$@CN	1M KOH	256	ACS Applied Materials & Interfaces, 11 (2019) 6890-6899[12]
Ni/Gd_2O_3/NiO	1M KOH	190	Journal of Colloid and Interface Science, 587 (2021) 457-466[13]
$Co(OH)_2$@P-NiCo-LDH	1M KOH	226	Journal of Colloid and Interface Science, 582 (2021) 535-542[14]
V Doped MoS_2	1M KOH	194	Applied Catalysis B: Environmental, 254 (2019) 432-442[15]
{111} faceted Ni_3S_2	1M KOH	189	Journal of Materials Chemistry A, 7 (2019) 18003-18011[16]
Ni_3S_2	**1M KOH**	**209**	**This work**
Ni_3S_2-Fe	**1 M KOH**	**206**	**This work**
Ni_3S_2-Fe-Ni	**1 M KOH**	**83**	**This work**

Table S2. A comparison of the HER performances of recently reported electrocatalysts in alkaline electrolytes.

Electrocatalysts	Electrolytes	Overpotential at 10 mA·cm^{-2} (mV)	
Fe_3C-Co nanoparticles	1M KOH	1.83	ACS Applied Materials & Interfaces, 12 (2020) 31552-31563.[17]
A-Ni-Fe Oxyphosphide	1M KOH	1.79	Advanced Functional Materials, 29 (2019) 1901949[18]
Co-Fe Oxyphosphide	1M KOH	1.69	ACS Sustainable Chemistry & Engineering, 9 (2021) 9436-9443[19]
NiS/NiP_2	1M KOH	1.69	Advanced Science, 6 (2019) 1900576[20]
$NixCo_3$-xO4/Ti_3C_2	1M KOH	1.67	ACS Applied Materials & Interfaces, 10 (2018) 4689-4696[21]
MoS_2/NiS Yolk-shell	1M KOH	1.66	ACS Applied Materials & Interfaces, 13 (2021) 34308-34319[22]
5-Pt/Ni/NF	1M KOH	1.64	Small, 15 (2019) 1803639[23]
MoS_2-NiS_2/NG	1M KOH	1.64	ACS Applied Energy Materials, 5 (2022) 2391-2399[24]
NiS_2/CeO_2	1M KOH	1.64	Materials Today Chemistry, 24 (2022) 100791[25]
NiS-NiS_2	1M KOH	1.63	Materials Today Energy, 23 (2022) 100906[26]
Ni_3S_2-Fe-Ni	**1 M KOH**	**1.55**	**This work**

Table S3. A comparison of the overall water splitting performances of recently reported electrocatalysts in alkaline electrolytes.

Electrochemical Measurements

The electrochemical tests were conducted at room temperature (20°C) using a CHI 760E workstation equipped with a standard three-electrode system in a 1 M KOH electrolyte to measure electrocatalytic properties. The working electrode utilized Ni_3S_2-Fe-Ni as a synchronizer, while the counter electrode was a platinum sheet and the reference electrode was Ag/AgCl (3 M KCl). The electrochemical tests were conducted at room temperature (25°C) using a CHI 760E workstation equipped with a standard three-electrode system in a 1 M KOH electrolyte to measure electrocatalytic properties. The capacitive current decreased when scanned at a rate of 1 mV/s, compensated for iR, within the range of -2 to 1. The complete linear scanning voltammetry (LSV) traits of the tests were documented, and the outputs were adjusted applying the Nernst equation, as calculated under here.

$$E(vs.RHE) = E(vs.Ag/AgCl) + (\frac{0.0592}{n})\lg\frac{C^0}{C_\alpha^0}$$

$$4OH^- - 4e^- = O_2 + H_2O$$

$$2H^+ + 2e^- = H_2$$

$$PH = -\lg[H^+] = \lg\frac{1}{[H^+]}$$

$$E(vs.RHE) = E(vs.Ag/AgCl) + (0.0592) * PH$$

$$E_{HER}(vs.RHE) = E(vs.Ag/AgCl) + 1.023$$

Based on the oxygen reduction reaction, the starting potential of the OER is 1.23 V

$$E_{OER}(vs.RHE) = E(vs.Ag/AgCl) + 1.023 - 1.23 = E(vs.Ag/AgCl) - 0.207$$

The Tafel analysis utilises the logarithm of the absolute overpotential (A) value post Nernst calibration as its horizontal coordinate. Cyclic voltammetry (CV) was used to determine the electrochemical double layer capacitance (Cdl) in the non-Faraday range (0.12 - 0.22 V vs. RHE), which was then used to evaluate the electrochemically active surface area (ECSA) of the samples. The scan rates for CV ranged from 20 mV/s to 120 mV/s, incremented by 20 mV/s. Various scan rates were employed to measure current densities. The vertical coordinate was set at 0.2 V, and the horizontal coordinate at the scanning rate. A plot was generated to illustrate the correlation between scanning rate and current density. The EIS frequency range covered the 100 kHz to 0.01 Hz range. The efficiency of water splitting in the system was measured using a dual-electrode setup, with the cathode and anode performed by Ni_3S_2-Fe-Ni electrodes, respectively.

References

[1] M. Yu, Z. Wang, J. Liu, F. Sun, P. Yang, J. Qiu, A hierarchically porous and hydrophilic 3D nickel–iron/MXene electrode for accelerating oxygen and hydrogen evolution at high current densities, Nano Energy. 63 (2019) 103880.
[2] Z. Li, M. Shao, H. An, Z. Wang, S. Xu, M. Wei, D.G. Evans, X. Duan, Fast electrosynthesis of Fe-containing layered double hydroxide arrays toward highly efficient electrocatalytic oxidation reactions, Chemical Science. 6 (2015) 6624–6631.
[3] Y. Wang, S. Tao, H. Lin, G. Wang, K. Zhao, R. Cai, K. Tao, C. Zhang, M. Sun, J. Hu, B. Huang, S. Yang, Atomically targeting NiFe LDH to create multivacancies for OER catalysis with a small organic anchor, Nano Energy. 81 (2021) 105606.
[4] Y. Wang, M. Qiao, Y. Li, S. Wang, Tuning Surface Electronic Configuration of NiFe LDHs Nanosheets by Introducing Cation Vacancies (Fe or Ni) as Highly Efficient Electrocatalysts for Oxygen Evolution Reaction, Small. 14 (2018).
[5] Y. Jia, L. Zhang, G. Gao, H. Chen, B. Wang, J. Zhou, M.T. Soo, M. Hong, X. Yan, G. Qian, J. Zou, A. Du, X. Yao, A Heterostructure Coupling of Exfoliated Ni–Fe Hydroxide Nanosheet and Defective Graphene as a Bifunctional Electrocatalyst for Overall Water Splitting, Advanced Materials. 29 (2017).
[6] M. Zhang, Y. Liu, B. Liu, Z. Chen, H. Xu, K. Yan, Trimetallic NiCoFe-Layered Double Hydroxides Nanosheets Efficient for Oxygen Evolution and Highly Selective Oxidation of Biomass-Derived 5-Hydroxymethylfurfural, ACS Catalysis. 10 (2020) 5179–5189.
[7] H. Zhang, X. Li, A. Hähnel, V. Naumann, C. Lin, S. Azimi, S.L. Schweizer, A.W. Maijenburg, R.B. Wehrspohn, Bifunctional Heterostructure Assembly of NiFe LDH Nanosheets on NiCoP Nanowires for Highly Efficient and Stable Overall Water Splitting, Advanced Functional Materials. 28 (2018).
[8] Z. Yu, K. Yao, S. Zhang, Y. Liu, Y. Sun, W. Huang, N. Hu, Morphological and reactive optimization of g-C_3N_4-derived Co,N-codoped carbon nanotubes for hydrogen evolution reaction, New Journal of Chemistry. 45 (2021) 6308–6314.
[9] L. Gong, X. Mu, Q. Li, L. Ma, Y. Xiong, R. Li, Rational design of Ni-induced NC @Mo_2C@MoS_2 sphere electrocatalyst for efficient hydrogen evolution reaction in acidic and alkaline media, International Journal of Hydrogen Energy. 46 (2021) 5250–5258.
[10] Y. Cao, Y. Meng, S. Huang, S. He, X. Li, S. Tong, M. Wu, Nitrogen-, Oxygen- and Sulfur-Doped Carbon-Encapsulated Ni_3S_2 and NiS Core–Shell Architectures: Bifunctional Electrocatalysts for Hydrogen Evolution and Oxygen Reduction Reactions, ACS Sustainable Chemistry & Engineering. 6 (2018) 15582–15590.
[11] A. Hanan, M. Ahmed, M.N. Lakhan, A.H. Shar, D. Cao, A. Asif, A. Ali, M. Gul, Novel rGO@Fe_3O_4 nanostructures: An active electrocatalyst for hydrogen evolution reaction in alkaline media, Journal of the Indian Chemical Society. 99 (2022) 100442.
[12] L. Yu, Y. Xiao, C. Luan, J. Yang, H. Qiao, Y. Wang, X. Zhang, X. Dai, Y. Yang, H. Zhao, Cobalt/Molybdenum Phosphide and Oxide Heterostructures Encapsulated in N-Doped Carbon Nanocomposite for Overall Water Splitting in Alkaline Media, ACS Applied Materials & Interfaces. 11 (2019) 6890–6899.

[13] H.H. El-Maghrabi, A.A. Nada, M.F. Bekheet, S. Roualdes, W. Riedel, I. Iatsunskyi, E. Coy, A. Gurlo, M. Bechelany, Coaxial nanofibers of nickel/gadolinium oxide/nickel oxide as highly effective electrocatalysts for hydrogen evolution reaction, Journal of Colloid and Interface Science. 587 (2021) 457–466.
[14] N. Song, S. Hong, M. Xiao, Y. Zuo, E. Jiang, C. Li, H. Dong, Fabrication of Co(Ni)-P surface bonding states on core–shell $Co(OH)_2$@P-NiCo-LDH towards electrocatalytic hydrogen evolution reaction, Journal of Colloid and Interface Science. 582 (2021) 535–542.
[15] S. Bolar, S. Shit, J.S. Kumar, N.C. Murmu, R.S. Ganesh, H. Inokawa, T. Kuila, Optimization of active surface area of flower like MoS2 using V-doping towards enhanced hydrogen evolution reaction in acidic and basic medium, Applied Catalysis B: Environmental. 254 (2019) 432–442.
[16] L. Li, C. Sun, B. Shang, Q. Li, J. Lei, N. Li, F. Pan, Tailoring the facets of Ni_3S_2 as a bifunctional electrocatalyst for high-performance overall water-splitting, Journal of Materials Chemistry A. 7 (2019) 18003–18011.
[17] K. Srinivas, Y. Chen, B. Wang, B. Yu, X. Wang, Y. Hu, Y. Lu, W. Li, W. Zhang, D. Yang, Metal–Organic Framework-Derived NiS/Fe_3O_4 Heterostructure-Decorated Carbon Nanotubes as Highly Efficient and Durable Electrocatalysts for Oxygen Evolution Reaction, ACS Applied Materials & Interfaces. 12 (2020) 31552–31563.
[18] C.C. Yang, S.F. Zai, Y.T. Zhou, L. Du, Q. Jiang, Fe_3C-Co Nanoparticles Encapsulated in a Hierarchical Structure of N-Doped Carbon as a Multifunctional Electrocatalyst for ORR, OER, and HER, Advanced Functional Materials. 29 (2019).
[19] J. Chen, Z. Guo, Y. Luo, M. Cai, Y. Gong, S. Sun, Z. Li, C.-J. Mao, Engineering Amorphous Nickel Iron Oxyphosphide as a Highly Efficient Electrocatalyst toward Overall Water Splitting, ACS Sustainable Chemistry & Engineering. 9 (2021) 9436–9443.
[20] P. Zhang, X.F. Lu, J. Nai, S. Zang, X.W. (David) Lou, Construction of Hierarchical Co–Fe Oxyphosphide Microtubes for Electrocatalytic Overall Water Splitting, Advanced Science. 6 (2019).
[21] X. Xiao, D. Huang, Y. Fu, M. Wen, X. Jiang, X. Lv, M. Li, L. Gao, S. Liu, M. Wang, C. Zhao, Y. Shen, Engineering NiS/Ni_2P Heterostructures for Efficient Electrocatalytic Water Splitting, ACS Applied Materials & Interfaces. 10 (2018) 4689–4696.
[22] P. Xu, H. Wang, J. Liu, X. Feng, W. Ji, C.-T. Au, High-Performance Ni_xCo_3-xO_4/Ti_3C_2Tx-HT Interfacial Nanohybrid for Electrochemical Overall Water Splitting, ACS Applied Materials & Interfaces. 13 (2021) 34308–34319.
[23] Q. Qin, L. Chen, T. Wei, X. Liu, MoS_2/NiS Yolk–Shell Microsphere-Based Electrodes for Overall Water Splitting and Asymmetric Supercapacitor, Small. 15 (2018).
[24] S. Battiato, L. Bruno, A. Terrasi, S. Mirabella, Superior Performances of Electroless-Deposited Ni–P Films Decorated with an Ultralow Content of Pt for Water-Splitting Reactions, ACS Applied Energy Materials. 5 (2022) 2391–2399.

[25] W.Y. Liao, W.D.Z. Li, Y. Zhang, Sulfur and oxygen dual vacancies manipulation on 2D NiS_2/CeO_2 hybrid heterostructure to boost overall water splitting activity, Materials Today Chemistry. 24 (2022) 100791.
[26] Y. Li, T. Dai, Q. Wu, X. Lang, L. Zhao, Q. Jiang, Design heterostructure of NiS–NiS_2 on NiFe layered double hydroxide with Mo doping for efficient overall water splitting, Materials Today Energy. 23 (2022) 100906.